

ENTRAINMENT AND SUBGRID LENGTHSCALES IN LARGE-EDDY SIMULATIONS OF ATMOSPHERIC BOUNDARY-LAYER FLOWS

BJORN STEVENS, C-H. MOENG AND P. P. SULLIVAN
National Center for Atmospheric Research
Boulder CO, USA 80307-3000

Abstract. The effect of the model for the lengthscale in sub-grid scale (SGS) parameterizations used in large-eddy simulations (LES) of atmospheric flows is considered. SGS models that carry predictive equations for SGS energy (i.e., \mathcal{T} models) are more susceptible to the model for the SGS lengthscale than are models that diagnose SGS energy, this is because in \mathcal{T} models most of the SGS buoyancy flux in the entrainment zone is found to be associated with Richardson numbers greater than unity, i.e., regimes where the equilibrium value of SGS energy is zero. We also show that the sensitivity of LES to the model of the lengthscale depends on the type of flow, and in particular the strength of the capping inversion. The lengthscale sensitivity of \mathcal{T} models is fruitfully interpreted using analytic solutions to the SGS energy equation for conditions of no transport and fixed forcing.

1. Introduction

At the heart of Large-Eddy Simulation (LES) is a separation between “resolved” and un-resolved scales. The former are solved for explicitly, and the effects of the latter (on the former) are modeled with a sub-grid scale (SGS) model. In studies of very high Reynolds number flows [such as those characteristic of the planetary boundary layer (PBL)] the class of SGS models commonly used involve the specification of some lengthscale l . Traditionally this lengthscale is taken to be equivalent to the size of the grid mesh Δ , e.g., Lilly (1967), thus making it commensurate with the implied boundary between the resolved and unresolved scales for a given numerical mesh.

¹The first author would like to acknowledge the Advanced Study Program at NCAR for support, as well as fruitful conversations with M. vanZanten and E. Saiki.

Deardorff (1980) proposed that in stably stratified flows l should be reduced, which implies that SGS motions operate at scales significantly smaller than Δ . Along with this stability contracted lengthscale he proposed a number of other changes (which we review in §2) to a form of the SGS model that solves a prognostic equation for the SGS energy and diagnoses other SGS quantities. Deardorff’s approach has been largely adopted by the atmospheric science community, although with a few exceptions his proposed changes have not been systematically investigated.

An exception is Schumann (1991), who studied in some detail Deardorff’s lengthscale corrections. In particular he compared three models: one in which no lengthscale correction was made; one in which the lengthscale correction proposed by Deardorff was made; and a third in which the lengthscale appearing in the eddy diffusivity was contracted for the case of vertical diffusion in the presence of stability. In coarse, $O(40^3)$, resolution studies of the weakly-capped convective boundary layer (CBL) Schumann found that the overall sensitivity of a calculation to these types of changes was relatively weak.

In contrast to Schumann, our experience has been that some elements of the solution are very sensitive to the SGS model. For instance, Sullivan et al., (1994) note that the stability reduction in the lengthscale “is a necessary ingredient in order to model PBL flows with strong capping inversions.” Similarly at the 4th GEWEX cloud-system studies workshop held in Seattle in August of 1997, one of us (CHM) showed that simulations of trade cumulus are quite sensitive to the stability correction of the SGS lengthscale. LES of the very stable boundary layer (E. Saiki personal communication 1998) also seem to require the lengthscale modification to preserve the strong inversion capping the outer (or residual) layer. Lastly, Stevens et al., (1999) note that for simulations of a strongly-capped smoke cloud “entrainment rates and SGS fluxes are dramatically altered” in the absence of a length scale correction in the TKE model, but that the Smagorinsky model is not commensurately sensitive to the model for the lengthscale.

In this paper we revisit these issues. After reviewing the theoretical basis for our inquiry in §2, and introducing our methods in §3, we reconcile the results of Schumann (1991) with our experiences (by examining how different flows react to the presence or absence of a stability correction to the SGS lengthscale) in §4. In §5 we show how the different sensitivity of the TKE and Smagorinsky models to the lengthscale formulation reflect non-equilibrium effects in the TKE budget, and how this behavior can be understood by considering analytic solutions to a local form of the TKE equation in conditions of constant forcing. Section §6 concludes with a summary and outlook.

2. Theoretical Background

As discussed in the introduction, LES explicitly solves for the large scales in the flow, but models the effect of unresolved motions on the resolved, large-scale, turbulent motions. Thus one must have a model of how these small scales behave, and this model must be written down in terms of the resolved scale variables at hand. Namely, one must derive a model of the SGS stresses $\tau_{ij} = \overline{u_i u_j} - \bar{u}_i \bar{u}_j$ and scalar fluxes, e.g., $\overline{u_i \theta} - \bar{u}_i \bar{\theta}$. The overbar represents a low-pass filtering with cutoff wavenumber of about Δ^{-1} thereby delineating the resolved component of a field.

In solving for the SGS stresses and fluxes, one can make the additional assumption that the averaging operation obeys Reynolds averaging rules; that is, for $u'_i \equiv u_i - \bar{u}_i$ then $\tau_{ij} = \overline{u'_i u'_j}$. Not unexpectedly, the second order equations (describing the evolution of the SGS covariances) provide a nice starting point for understanding contemporary SGS parameterizations used in LES of the PBL (Lilly, 1967; Deardorff, 1973b). In particular it is worthwhile to consider three of the second order equations: First, the equation for $e = \frac{1}{2} \delta_{ij} \tau_{ij}$, the SGS turbulent kinetic energy,

$$\frac{\partial e}{\partial t} = -\frac{\partial}{\partial x_k} (\bar{u}_k e) - \bar{a}_{ij} \frac{\partial \bar{u}_i}{\partial x_j} - \frac{\partial}{\partial x_k} \left(\overline{u'_k e} + \frac{1}{\rho_0} \overline{u'_k p'} \right) + \frac{g}{\Theta_0} \overline{u'_3 \theta'} - \epsilon; \quad (1)$$

where we have introduced $\bar{a}_{ij} = \left(\tau_{ij} - \frac{2}{3} \delta_{ij} e \right)$ to denote the anisotropic component of the stress, its evolution proceeds according to

$$\begin{aligned} \frac{\partial \bar{a}_{ij}}{\partial t} = & -\frac{\partial}{\partial x_k} (\bar{u}_k \bar{a}_{ij}) - \bar{a}_{ik} \frac{\partial \bar{u}_j}{\partial x_k} - \bar{a}_{jk} \frac{\partial \bar{u}_i}{\partial x_k} - \frac{2}{3} e D_{ij} + \frac{\delta_{ij}}{3} \bar{a}_{kl} D_{kl} \\ & - \frac{\partial}{\partial x_k} \left(\overline{u'_k a_{ij}} \right) + \frac{g}{\Theta_0} \left(\delta_{i3} \overline{u'_j \theta'} + \delta_{j3} \overline{u'_i \theta'} - \frac{2}{3} \delta_{ij} \overline{u'_3 \theta'} \right) \\ & - \frac{1}{\rho_0} \left[\frac{\partial}{\partial x_j} (\overline{u'_i p'}) + \frac{\partial}{\partial x_i} (\overline{u'_j p'}) \right] + \frac{1}{\rho_0} \left[p' \left(\frac{\partial u'_j}{\partial x_i} + \frac{\partial u'_i}{\partial x_j} \right) \right], \quad (2) \end{aligned}$$

(where $D_{ij} = \partial \bar{u}_i / \partial x_j + \partial \bar{u}_j / \partial x_i$ denotes the resolved scale deformation). The third equation is for, $\overline{u'_i \theta'}$, the SGS buoyancy (or heat) flux (because we only consider dry flows here, the potential temperature θ is the relevant buoyancy variable),

$$\begin{aligned} \frac{\partial}{\partial t} (\overline{u'_i \theta'}) = & -\frac{\partial}{\partial x_k} (\bar{u}_k \overline{u'_i \theta'}) - \left(\bar{a}_{ik} + \frac{2}{3} \delta_{ik} e \right) \frac{\partial \bar{\theta}}{\partial x_k} - \overline{u'_k \theta'} \frac{\partial \bar{u}_i}{\partial x_k} \\ & - \frac{\partial}{\partial x_k} (\overline{u'_i u'_k \theta'}) + \frac{1}{\rho_0} p' \frac{\partial \theta'}{\partial x_i} - \frac{1}{\rho_0} \frac{\partial}{\partial x_i} (\overline{p' \theta'}) + \delta_{i3} \frac{g}{\Theta_0} \overline{\theta'^2}. \quad (3) \end{aligned}$$

To complete the relevant set of second order equations one must also consider the equation for $\overline{\theta'^2}$. However, the variance production term in (3) is neglected in the class of SGS models we consider, thus allowing us to truncate the second order equations to the above set. As is well known, irrespective of the $\overline{\theta'^2}$ equation, the set of second order equations is not closed. Their closure requires that the unknown terms (e.g., the dissipation, and the triple moment terms) must be modeled.

2.1. SGS MODELS

Over the years there have been a variety of SGS models proposed (and used), based on simpler and more elaborate representations of the above system of equations. Most of the more elaborate closures date back to the early years of LES (Deardorff, 1973a; Deardorff, 1973b; Sommeria, 1976; Schemm and Lipps, 1973; Schumann, 1991; Schmidt and Schumann, 1989). More recently, and in the absence of clearly superior alternatives, most LES groups choose to use as much grid resolution as possible in conjunction with a very simple representation of the second order equations—particularly for convectively forced flows. It is these very simple parameterizations that we wish to discuss. Starting our discussion from the point of view of the second order equations serves the purpose of emphasizing just how simple these commonly used parameterizations are.

Specifically, we can derive the relevant class of SGS models by starting from (2) and (3) above and assuming that the primary balance in each equation is between pressure fluctuations and isotropic production, and furthermore assuming that the pressure-fluctuation correlation terms can be modeled:

$$\frac{1}{\rho_0} \left[p' \left(\frac{\partial u'_j}{\partial x_i} + \frac{\partial u'_i}{\partial x_j} \right) \right] = -c_m \frac{e}{l} \overline{a}_{ij}, \quad \text{and} \quad \frac{1}{\rho_0} \overline{p' \frac{\partial \theta'}{\partial x_i}} = -c_h \frac{e}{l} \overline{u'_i \theta'}. \quad (4)$$

In (4) we have introduced some constants c_h , c_m (and subsequently c_e); if one assumes a filter-scale in an energy inertial-subrange, their values can be derived explicitly (Lilly, 1967; Moeng and Wyngaard, 1989; Schmidt and Schumann, 1989; Schumann, 1991). A lengthscale l also shows up in (4). An evaluation of different models of l is the primary objective of this study.

If in (2) and (3) we use the models of the pressure terms given by (4) and neglect everything else except the isotropic production terms, we obtain as a zeroth order balance a simple diagnostic relation between the desired SGS quantities and the resolved flow:

$$\overline{a}_{ij} = -K_m D_{ij}, \quad \text{and} \quad \overline{u'_i \theta'} = -K_h \frac{\partial \overline{\theta}}{\partial x_i}, \quad (5)$$

where the SGS exchange coefficients $K_m = c_m l \sqrt{e}$ and $K_h = c_h l \sqrt{e}$ can be thought of as an eddy viscosity and an eddy diffusivity respectively. If one further assumes that the third moment terms in (1) behave in a down gradient fashion (i.e., $\overline{u'_k(e + p'/\rho_0)} = -2K_m \partial e / \partial x_k$) and that the dissipation takes the form $\epsilon = c_\epsilon e^{3/2} / l$ then (1) takes on a somewhat simpler form:

$$\frac{\partial e}{\partial t} = -\frac{\partial}{\partial x_k} (\overline{u_k} e) + \frac{\partial}{\partial x_k} \left(2K_m \frac{\partial e}{\partial x_k} \right) + K_m S^2 - K_h N^2 - c_\epsilon \frac{e^{3/2}}{l}, \quad (6)$$

where we have introduced the symbols S^2 and N^2 to respectively represent the square deformation and the stability of the flow,

$$S^2 = \frac{\partial \overline{u}_i}{\partial x_j} D_{ij} \quad \text{and} \quad N^2 = \frac{g}{\Theta_0} \frac{\partial \overline{\theta}}{\partial x_3}. \quad (7)$$

Upon specification of l , (6) and (5) form a closed system of equations that underlies the SGS model known as the TKE model (Lilly, 1967; Deardorff, 1973b; Deardorff, 1980) which we denote by \mathcal{T} .

The Smagorinsky model can be interpreted as the limiting form of \mathcal{T} that results if one neglects the transport, third moment and time rate-of-change terms in (6). For a given form for l these simplifications allow one to solve for the SGS energy diagnostically:

$$e = \frac{c_m}{c_\epsilon} (lS)^2 \left(1 - \frac{c_h}{c_m} Ri \right), \quad \text{where} \quad Ri \equiv \frac{N^2}{S^2} \quad (8)$$

From (8) and the definition of the SGS exchange coefficients it follows that

$$K_m = (c_s l)^2 S \sqrt{1 - \frac{c_h}{c_m} Ri}, \quad K_h = \frac{c_h}{c_m} K_m, \quad \text{and} \quad c_s = \left(\frac{c_m^3}{c_\epsilon} \right)^{1/4}. \quad (9)$$

Generically (8) and (9) shall be referred to as \mathcal{S} , or the \mathcal{S} -model; in the special case (corresponding to the traditional Smagorinsky model) where l is set equal to the size of the grid mesh, Δ , we refer to (8) and (9) as \mathcal{S}_δ , or as the the \mathcal{S}_δ -model. Two further features of the \mathcal{S} model are worth noting here. First, the ratio c_m/c_h nominally has two physical interpretations: it is a cutoff Richardson number on the one hand, and an eddy Prandtl number on the other. Second, the diagnostic relation (8) represents only one root of the original equation, and thus is only valid for $Ri \leq c_m/c_h$; for $Ri > c_m/c_h$ we choose $e = K_m = K_h = 0$, in accord with the other root of the governing system.

2.2. LENGTH-SCALE MODELS

Although the \mathcal{S} model is usually implemented with $l = \Delta$, most implementations of \mathcal{T} stem from Deardorff's work with stratocumulus, for which he

proposed a new stability related length-scale $l_s = c_l \sqrt{e} N^{-1}$ and further specified

$$l = \min(l_s, \Delta), \quad \text{and} \quad c_h \rightarrow c_{h1} + \frac{c_{h2}l}{\Delta}, \quad c_\epsilon \rightarrow c_{\epsilon1} + \frac{c_{\epsilon2}l}{\Delta}. \quad (10)$$

Deardorff chose $c_l = 0.76$, although Schumann later argued that if $c_l \sqrt{e}$ is to be interpreted as the RMS value of w' , then for isotropic conditions $c_l = \sqrt{2/3}$. The set of relations given in (10) shall be collectively referred to as the stability modified lengthscale model and denoted by σ to distinguish it from the uncorrected lengthscale model ($l = \Delta$), which we denote by δ . It appears that σ is the simplest set of modifications that can be made to \mathcal{T} that allow its diagnostic limit (i.e., \mathcal{S}) to have both a Prandtl number that increases with stability and a Richardson number cut-off.² The additional constants are specified such that the Prandtl number increases with stability in a reasonable fashion, and so that the cut-off Richardson number takes on a plausible value.

Applying (10) to the system \mathcal{S} , results in a new model, which we call \mathcal{S}_σ :

$$e = \frac{c_m c_l \Delta^2 S^2}{\tilde{c}_\epsilon Ri} \left(1 - \frac{Ri}{Ri_c}\right)^2, \quad \text{where} \quad Ri_c = \frac{c_m}{\tilde{c}_h}, \quad (11)$$

and

$$K_m = \left(\frac{(c_m c_l)^3}{\tilde{c}_\epsilon^2}\right) \Delta^2 S \frac{1}{Ri^{3/2}} \left(1 - \frac{Ri}{Ri_c}\right)^2, \quad (12)$$

$$K_h = \left[\frac{c_{h1}}{c_m} + \left(\frac{c_l^2 c_{h2}}{\tilde{c}_\epsilon Ri}\right) \left(1 - \frac{Ri}{Ri_c}\right)\right] K_m, \quad (13)$$

where, we have defined additional constants,

$$\tilde{c}_\epsilon = c_{\epsilon2} + c_{h2} c_l^2 \quad \text{and} \quad \tilde{c}_h = \frac{c_{\epsilon1}}{c_l^2} + c_{h1}. \quad (14)$$

Equations (11)-(13) are only appropriate for $l_s \leq \Delta$, and $Ri < Ri_c$. It is straight forward to show that $l_s = \Delta$ at $Ri = Ri_\sigma \equiv c_l^2 c_m / (c_\epsilon + \tilde{c}_h c_l^2)$ (where for our choice of constants $Ri_\sigma \approx 0.06$.) Consequently the system (11)-(13) applies for $Ri_\sigma \leq Ri \leq Ri_c$. For $Ri > Ri_c$ we set e to zero while for $Ri < Ri_\sigma$ we use (8) and (9). Also note that the \mathcal{S}_δ and the \mathcal{S}_σ models have (for typical values of constants) slightly different cut-off Richardson

²The cut-off Richardson number, considered desirable by some authors (Deardorff, 1973b; Sommeria, 1976), has been criticized by others on the grounds that it typically implies that the SGS model violates realizability. However, recognizing that the equilibrium equation for e actually has two roots avoids this problem.

numbers (i.e., 0.23 vs 0.33), but as we show later, this is not a critical difference. An undesirable aspect of the σ model is its lack of continuity at $Ri = Ri_\sigma$ in derivatives of e , K_m and K_h — although this is readily remedied by using a geometric mean to match the lengthscales instead of a *min* function in (10).

In summary, we have a description of four types of models, respectively the \mathcal{T}_σ , \mathcal{T}_δ , \mathcal{S}_σ , and \mathcal{S}_δ models, where the notation follows directly from the discussions above.

3. Calculations

The simulations discussed in this paper are based on the code described by Stevens et al., (1999). To recap, the code is an anelastic, finite difference code that can use any of the SGS models described above. For the constants ($c_m, c_{h1}, c_{h2}, c_{\epsilon1}, c_{\epsilon2}, c_l$) we use the values (0.1, 0.1, 0.2, 0.225, 0.705, 0.82). All calculations are performed on a regular 96^2 doubly periodic grid in the horizontal with $\Delta x = \Delta y = 33m$ with free-slip boundary conditions. The vertical grid has a base value of 25m but is gradually contracted to be a constant value of either 5m (for runs forced by radiative cooling) or 10m (for calculations forced with a surface heat flux) in a zone of depth Δ_z spanning the inversion. Above this zone it is gradually stretched.

We consider two types of initial profiles and two types of forcing. For the forcing, in what we call CBL calculations we specify a constant surface heat flux of 60 Wm^{-2} , and in what we call SMK calculations we drive the turbulence by cooling through radiative flux divergence (of up to 60 Wm^{-2}) in a narrow zone at the top of a smoke layer. The initial temperature profiles all are neutrally stratified with $\theta = 288K$ below 687.5m, but differ in the stability characteristics of the capping layer. One type of initial capping layer is a layer of constant stability, that meets the well mixed layer without any intervening enhancement in the stability; the other is only very weakly stable, but is separated from the neutrally stratified underlying fluid by a sharply stratified transition layer — in which θ increases linearly (by the value $\Delta\Theta_v$) over 25m. In all cases the lower layer is filled with a tracer whose mixing ratio is unity below 687.5 m and decreases linearly to its value of zero at $z \geq 712.5m$. In the case of the radiatively forced simulations this tracer acts as the radiatively active substance necessary to generate radiative cooling (Stevens et al., 1999).

Calculations are only analyzed once they reach a quasi-steady state (as measured by the linearity of the fluxes of conserved variables). The length of the analysis for different calculations is indicated in Table 1. Unless otherwise noted averages (denoted by angle brackets) are over x, y , and t . In the interests of generality quantities are normalized by the governing

TABLE 1. Parameters for different experiment types: Jump in theta in the initial conditions, $\Delta\Theta$; lapse rate in upper layer, γ ; type of forcing; Depth of contracted vertical mesh, Δ_z ; total time of run, t_f ; period over which the analysis takes place t_a ; non-dimensional parameters for the control runs (which are based on the \mathcal{T}_σ SGS model);

Name	$\Delta\Theta$	γ	Forcing	$\Delta_z[m]$	t_f/t_*	t_a/t_*	$w_* [\text{ms}^{-1}]$	$z_* [n]$
CBL-,	n/a	6.0	Surface Flux	400	8.8	2.2	1.12	921
CBL	4 K	0.1	Surface Flux	200	10.3	2.6	1.04	725
SMK	2 K	0.1	Radiation	100	13.3	4.4	0.96	779

non-dimensional parameters of the flow: z_* , w_* and Q_* . Here we define $w_*^3 = 2.5B$ where B is the integral (from 0 to z_*) of the buoyancy production term in the TKE equation. For historical reasons (and because the entrainment flux is not always one fifth of the surface flux in the CBL) we allow the definition of Q_* to depend on the flow: For CBL flows we take Q_* equal to the surface buoyancy flux; for the SMK flows we define $Q_* = w_*^3 \Theta_0 / (gz_*)$. The height of the inversion z_* is defined as in Sullivan et al., (1998) to be the average height at any given time of the maximum value of N^2 . The analysis procedure is the same as in Stevens et al. (1999) in that some calculations are branched from intermediate states of other calculations, however all simulations are allowed some time to develop independence from the control before they are analyzed. Most statistics are accumulated at 30s intervals during the course of a calculation, although some diagnostics are computed, in a post-processing sense, from a six-fold sparser set of 3D volumes. The sensitivity of our results to both our analysis procedure and our method of grid-stretching in the vertical has been thoroughly examined, and found not to be an issue.

4. Results

Figure 1 illustrates the sensitivity of the three different flows of Table 1 to the formulation of l in the SGS model \mathcal{T} . Panel (a) is for a flow (CBL-, γ) similar to that investigated by Schumann (although our capping layer is twice as stable as the Schumann case it has the same structure). In this flow, the effect of the σ model is relatively minor and similar in character to that reported by Schumann (1991).

The effects of the σ model become more pronounced as the capping inversion becomes stronger, e.g., panels (b) and (c). In both the CBL and SMK calculations, sensitivities of the SGS fluxes to the model for l also

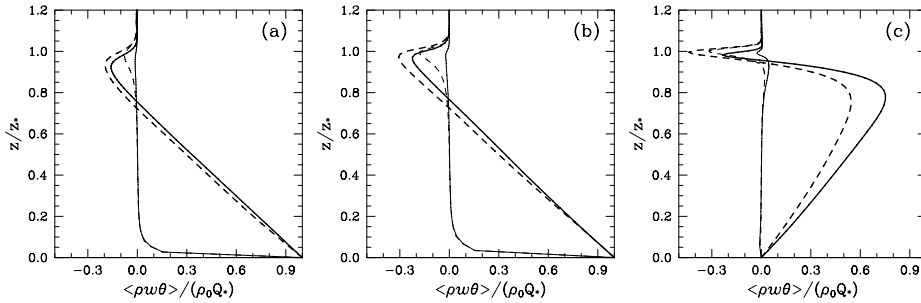


Figure 1. Non-dimensional heat fluxes from integrations CBL-, , CBL and SMK. Solid lines are from calculations with the \mathcal{T}_σ model and dashed lines are from calculations with the \mathcal{T}_δ model. Thick lines denote the total flux and thin lines denote SGS component of total flux. Note that in panel (c) the scaling of the runs depends on the flow, and so as to illustrate the nature of the sensitivity the scaling of the \mathcal{T}_δ calculation is done with the Q_* from the \mathcal{T}_σ calculation.

strongly impact the net (resolved plus SGS) fluxes — and hence the bulk energetics. Because the entrainment heat flux can be related to the entrainment rate ($w_e = dz_*/dt$), these effects are also reflected in the entrainment rates; in our three flows, when we replace the \mathcal{T}_σ by the \mathcal{T}_δ model, w_e increases by 4, 50, and 60 % for the CBL-, , CBL and SMK calculations respectively. The lack of a strict correspondence between the minimum heat flux near the inversion, and the entrainment rate, largely reflects the fact that the structure of the inversion (i.e., the thickness of the entrainment zone and the jumps of buoyancy across it) are also impacted by changes to the lengthscale model.

In terms of other effects, (apart from those that are not obvious consequences of changes to the overall energetics of the flow) we find that the σ model sharply increases the dissipation at the inversion, and modestly increases the maximum horizontal velocity variances (which peak just below z_*). The former result is in accord with Schumann’s analysis.

For a given type of forcing the sensitivity of the calculation to the model for l tends to increase with the strength of the capping inversion; however, for a given capping inversion SMK calculations appear more sensitive to the model for l than do CBL type calculations. Because of the differing nature of the flows (one driven by heating at its base the other driven by cooling at its top) at the time of the analysis $(\Delta\Theta)_{CBL}$ has decreased to 3.5 K and $(\Delta\Theta)_{SMK}$ has increased to about 2.4 K. Nonetheless, it is still true that $(\Delta\Theta)_{CBL} > (\Delta\Theta)_{SMK}$, yet the sensitivity of the SMK calculation to the lengthscale model remains greater. An examination of PDFs of the maximum column stability shows that $(\Delta\theta)_{CBL} > (\Delta\theta)_{SMK}$ is also true locally. Consequently the greater sensitivity of the SMK calculations probably re-

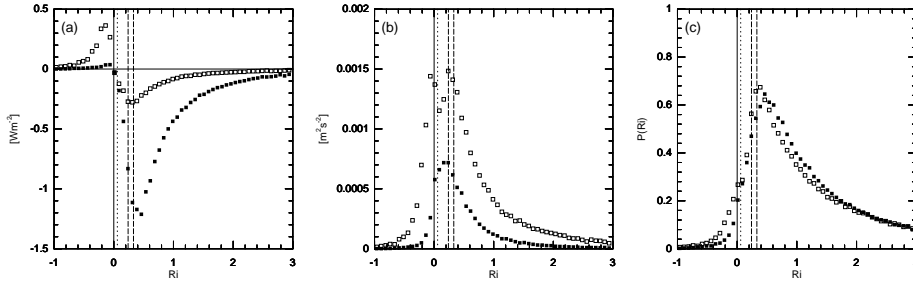


Figure 2. Statistics from the SMK flow during the analysis period at the level where the SGS buoyancy flux is a minimum: (a) net SGS buoyancy-flux occurring in binned Ri number intervals; (b) net SGS energy in the same interval; (c) probability distribution function of Ri . Also marked are the points Ri_σ and the values of Ri_c for the \mathcal{S}_σ and \mathcal{S}_δ model respectively.

flects their different dynamics. A point we shall return to subsequently.

5. Non-Equilibrium Effects

5.1. FLOW ANALYSIS

To better understand the differences among the SGS models we analyze the flow at the level associated with the minimum SGS buoyancy flux. In doing this we were interested in learning what portions of the flow contribute to the differences in the SGS fluxes. For instance, to what extent could the difference between the models be associated with different cut-off Richardson numbers, or different amounts of energy in the flow at Richardson numbers less than the cut-off Richardson number.

Fig. 2 illustrates the important results from this analysis for the SMK calculations. We have done an identical analysis for the CBL calculations and find broadly similar results. Most of the negative SGS buoyancy flux in both the \mathcal{T}_δ and \mathcal{T}_σ calculation is associated with very stable parts of the flow, i.e., $Ri > 0.5$. Moreover, the stability modified model, which has a smaller consumption of TKE through buoyancy effects, also maintains significantly larger amounts of energy in the flow. Both of these facts occur despite the fact that the large-scale structure of the outer flow is very similar when viewed in terms of the probability density of Richardson numbers.

At the level of the flow being analyzed in Fig. 2 most of the flow is at $Ri > Ri_\sigma$, indicating that the σ model of the lengthscale is being invoked most of the time. As we shall subsequently show, the σ model of the lengthscale tends to result in less rapid destruction of e than does the δ model. The fact that there is less dissipation for a given value of e is consistent with our earlier observation that the horizontal velocity variances are more peaked near the inversions for calculations with the σ model of the length-

scale, as well as the fact that the overall values of e in the \mathcal{T}_σ calculation are higher.

In accord with the above results are three further findings: First, simulations based on the \mathcal{S} model are about half as sensitive to the model for l . Second, transport (and transport-like) terms in the \mathcal{T} model can not explain the greater sensitivity of the \mathcal{T} model to the formulation of l ; the sensitivity remains in a SMK calculations for which the transport and transport like terms in the equation for e are eliminated. Third, in a calculation in which the timestep in the TKE equation is artificially contracted, so 10 TKE timesteps were computed for every dynamic timestep thereby allowing the TKE model to artificially approach equilibrium ten times faster, the sensitivity of the \mathcal{T} model to the formulation for l is greatly reduced. In summary we find that the \mathcal{T} model allows fossil TKE to exist and the rate at which it is dissipated, and/or converted to potential energy via mixing depends largely on the model of l . It turns out that we can be a great deal more precise in our analysis by considering analytic solutions to a simplified form of the TKE equation in regimes where $Ri > Ri_\sigma$.

5.2. ANALYTIC SOLUTIONS

Specifically we find it illuminating to analyze the behavior of the \mathcal{T} model in the absence of fluxes of e (i.e., neglecting the first two terms on the RHS of (6)) and for conditions of fixed forcing. The first assumption is justified by our observation that the sensitivity of the \mathcal{T} model is not affected by the absence of these term. The second assumption is made for convenience, but is reasonable for small e , or if the timescales for the large-scale flow are much larger than the timescales for e . These assumptions permit us to consider solutions to an equation of the form:

$$\frac{de}{dt} = K_m S^2 - K_h N^2 - c_\epsilon \frac{e^{3/2}}{l}. \quad (15)$$

The first and third terms on the RHS are positive definite and describe the production of e by shear and its destruction by dissipation respectively. The second term is the buoyancy term. It describes the exchange between potential and kinetic energy and can be either positive or negative.

We are interested in understanding how an initial value of energy will adjust to its equilibrium value in conditions when N^2 and S^2 (and by implication Ri) are fixed. Moreover, because we are interested in how the different models of l affect this adjustment to equilibrium, we here only consider situations in which $Ri > Ri_\sigma$, i.e., for the situation in which the σ model may be applied. Thus we have two equations, one for e_δ and another for e_σ that describe the evolution of e under the $l = \delta$ and $l = \sigma$ models

respectively:

$$\frac{de_\delta}{dt} = \Delta e^{1/2} S^2 (c_m - c_h Ri) - c_\epsilon \frac{e_\delta^{3/2}}{\Delta} \quad (16)$$

$$\frac{de_\sigma}{dt} = c_l \frac{e}{N} S^2 (c_m - \tilde{c}_h Ri) - \tilde{c}_\epsilon \frac{e_\sigma^{3/2}}{\Delta}, \quad (17)$$

The similarity between (16) and (17) can be misleading; implicit in the form of the constants \tilde{c}_h and \tilde{c}_ϵ , i.e., (14), is the fact that the second term on the RHS [which looks like the buoyancy term in (16)] is actually composed of two terms, one originating in the original SGS buoyancy term, and the other originating in the SGS dissipation term of (15). The same is true for the third term on the RHS.

Equations (16) and (17) are instructive in that they illustrate how the σ model of the lengthscale places the buoyancy terms on equal footing with dissipation. For small e the lowest power of e terms dominate the budget, and thus the c_h and \tilde{c}_h terms dominate the adjustment. When c_h dominates the adjustment to smaller values of e in (16) most of the excess e is given up to the potential energy field through the SGS buoyancy flux. In contrast, because $\tilde{c}_h = c_{h1} + c_{\epsilon1}/c_l^2$, the adjustment in (17) is due to both dissipation and buoyancy (actually the $c_{\epsilon1}$ term dominates). As we show later, these issues can be looked at more quantitatively by comparing the instantaneous and integrated buoyancy fluxes implied by the two models in their respective approach to equilibrium. But first we must consider how, under the two models of the lengthscale, the energy approaches its equilibrium value.

In general we are interested in all solutions to equations (16) and (17) given an initial amount of energy $e_0 > 0$. For $Ri > Ri_\sigma$ both (16) and (17) yield solutions in two regimes. In the first regime the equilibrium value of the energy is greater than zero and is given by (8) and (11) respectively. In the second regime the energy decays to zero. However, because $c_h \neq \tilde{c}_h$, there does exist a small range in Richardson numbers in which the models behave quite differently. Nonetheless, because the behavior of the models in this regime was previously shown to be most important to a simulation as a whole, we confine our subsequent analysis to the very stable, $Ri > c_m/c_h$, regime.

5.2.1. Time decay of e

For $Ri > c_m/c_h > c_m/\tilde{c}_h$, (16) and (17), yield the following solutions:

$$e_\delta(t) = \alpha \tan^2 \left[\arctan \left(\sqrt{\frac{e_0}{\alpha}} \right) - \frac{t}{2\tau} \right], \quad \tau = \frac{1}{\sqrt{S^2 c_\epsilon |c_h Ri - c_m|}} \quad (18)$$

$$e_\sigma(t) = \tilde{\alpha} \left[\frac{\sqrt{\frac{e_0}{\tilde{\alpha}}} \exp\left(\frac{-t}{\tilde{\tau}}\right)}{1 - \sqrt{\frac{e_0}{\tilde{\alpha}}} (\exp\left(\frac{-t}{\tilde{\tau}}\right) - 1)} \right]^2, \quad \tilde{\tau} = \frac{2}{S \frac{c}{\sqrt{Ri}} |\tilde{c}_h Ri - c_m|}, \quad (19)$$

where the parameters

$$\alpha = \frac{\Delta^2 S^2}{c_\epsilon} (c_h Ri - c_m), \quad \text{and} \quad \tilde{\alpha} = \frac{\Delta^2 S^2 c_l^2}{\tilde{c}_\epsilon Ri} (\tilde{c}_h Ri - c_m)^2 \quad (20)$$

can be interpreted as measures of how strongly the flow wants to damp out any ambient SGS energy.

These solutions quantitatively illustrate that the different models equilibrate e on different timescales. Specifically, $e_\delta \rightarrow 0$ in finite time, whilst e_σ adjusts exponentially. The tendency for the σ model to generate longer timescales is also characteristic of the $Ri_\sigma \leq Ri \leq c_m/\tilde{c}_h$ regime, in which case τ and $\tilde{\tau}$ are effective equilibration timescales. Overall we note that the dilation of the timescales is a reasonable effect, in that turbulence in the form of waves, or pancake-like vortices is thought to persist in stratified flows. However the tendency for $e_\sigma(t)$ to approach its fixed point in infinite time could be interpreted as meaning that under the σ model the flow can not cease to be turbulent (or relaminarize) in finite time.

5.2.2. The SGS buoyancy flux

Given our interest in the buoyancy flux associated with different models of l , we here evaluate the instantaneous SGS buoyancy flux \mathcal{B}_x^0 that a model x would produce for a given amount of energy. Specifically we consider the ratio $\mathcal{B}_\delta^0/\mathcal{B}_\sigma^0$ which is just the ratio of the terms in (16) and (17) associated with the SGS buoyancy flux:

$$\frac{\mathcal{B}_\delta^0}{\mathcal{B}_\sigma^0} = \frac{c_h}{\frac{l_s}{\Delta} \left(c_{h1} + \frac{l_s}{\Delta} c_{h2} \right)}. \quad (21)$$

Note that the denominator has two terms because a component of both the second and third terms on the RHS of (17) is due to the original buoyancy term. An analysis of $\mathcal{B}_\delta^0/\mathcal{B}_\sigma^0$ shows that it is greater than one, and for small e_0 (which is the typical scenario we consider) it goes as $\approx 3\Delta/l_s$ which is typically much larger than 1.

However, because the σ model significantly dilates the timescales for the adjustment of e it is not transparent that the σ model for l implies less total SGS buoyancy flux than does the δ model for l . To address this issue quantitatively we can solve for the time integrated buoyancy flux as the energy decays to its equilibrium value. Namely we are interested in solutions to

$$\mathcal{B}_x^\infty = \frac{g}{\Theta_0} \int_0^\infty \overline{w'\theta'} dt = N^2 \int_0^\infty K_h(t) dt \quad (22)$$

where $K_h(t) = c_h l \sqrt{\epsilon}$ is determined by choosing a particular model for c_h and l and the corresponding forms for $\epsilon(t)$. Also note that we are again assuming that the outer flow is frozen (i.e., N^2 is constant), this assumption begins to break down as timescales become longer, but the analysis is still instructive, in part because it seems to provide a plausible lower bound for the ratio of the buoyancy flux implied by the different models of l . Again the integration is straight forward, yielding

$$\mathcal{B}_\delta^\infty = \frac{-2c_h}{c_\epsilon} \Delta^2 N^2 \ln \left\{ \cos \left[\arctan \left(\sqrt{\frac{e_0}{\tilde{\alpha}}} \right) \right] \right\} \quad (23)$$

$$\begin{aligned} \mathcal{B}_\sigma^\infty &= c_l c_{h1} N \tilde{\tau} \tilde{\alpha} \left[\sqrt{\frac{e_0}{\tilde{\alpha}}} - \ln \left(1 + \sqrt{\frac{e_0}{\tilde{\alpha}}} \right) \right] \\ &\quad + \frac{c_l^2 c_{h2}}{\Delta} (\tilde{\alpha})^{3/2} \tilde{\tau} \left[\frac{e_0}{2\tilde{\alpha}} - \sqrt{\frac{e_0}{\tilde{\alpha}}} + \ln \left(1 + \sqrt{\frac{e_0}{\tilde{\alpha}}} \right) \right]. \end{aligned} \quad (24)$$

For the conditions we are interested in $e_0 \ll \tilde{\alpha}$, in which case (23) and (24) can be effectively approximated by their $O(\frac{e_0}{\tilde{\alpha}})$ expansions:

$$\mathcal{B}_\delta^\infty = \frac{c_h N^2 e_0}{S^2 (c_h Ri - c_m)} \quad \text{and} \quad \mathcal{B}_\sigma^\infty = \frac{c_{h1} N^2 e_0}{S^2 (\tilde{c}_h Ri - c_m)}. \quad (25)$$

The ratio $\mathcal{B}_\delta^\infty / \mathcal{B}_\sigma^\infty$ depends only on Ri ; for Richardson numbers of interest (i.e., $Ri \geq 0.4$) it is typically about 5. In the limit as $Ri \rightarrow \infty$ the ratio become simply \tilde{c}_h / c_{h1} , which for our choices of constants is about 4.3.

Typically these values are significantly less than $\mathcal{B}_\delta^0 / \mathcal{B}_\sigma^0$ but they are on the order of the differences in the SGS fluxes in the actual flows (e.g., Fig. 1), thus this calculation appears relevant, and provides further support for the idea that the chief difference resulting from the different models of l is in what they do to small amounts of energy leaked into stable regions of the flow. The fact that the SMK calculation is more sensitive to the model for l is consistent with the fact that in this calculation the sources of large-scale turbulence exist in very close proximity to the strong capping inversion; thus the idea that this flow would “leak” more energy into the inversion layer — and thus be more sensitive to the model for l — is a plausible one.

6. Summary and Outlook

We have shown that LES of PBL flows is sensitive to the formulation of the lengthscale in the SGS model. The sensitivity is more apparent in flows capped by strong (or step-like) inversions, and in flows driven by radiative cooling just under the base of the inversion layer. These results may explain why Schumann (who considered a very weakly capped flow driven by surface

heating) found a relatively weak sensitivity to the SGS model, and why Deardorff only introduced the stability corrected lengthscale when he began simulating stratocumulus.

In general the sensitivity affects the partitioning between the resolved and SGS component of the total buoyancy flux. Depending on the flow the overall entrainment flux can also change (in some cases significantly), although the degree of sensitivity of the net flux (SGS plus resolved) may depend on a variety of factors — including ones numerical methods. Because the partitioning between the resolved and SGS heat fluxes at the inversion is very sensitive to assumptions made in the SGS model, arguments (for instance about the degree to which a process is resolved) that are based on this partitioning are specious.

The sensitivity of the flow to the formulation of the lengthscale is most evident in models that predict the time-evolution of the SGS TKE. This result is traced to the fact that the additional mixing present when the lengthscale model is unmodified for stability is associated with very small amounts of fossil TKE that finds its way into very stably stratified regions of the flow. We derive analytic solutions to the TKE equation in the absence of transport or transport like terms which prove useful in understanding our results. In particular these derivations indicate that, in the absence of any compensating effects, non-equilibrium TKE results in at least 4-5 times as much mixing in the absence of stability modifications to the lengthscale model.

We hesitate to argue on behalf of one or the other SGS formulation. In part because we find the basic formulation problematic, and thus view all of the approaches skeptically. Heretofore, the greatest merit of any of the above discussed SGS formulations has been that the overall flow is not sensitive to the details. We show that in certain situations this is not true.

Although the \mathcal{T}_δ model of the lengthscale is attractive in that it is simple and has nice convergence properties (actually it must because the mixing is tied to the grid in a way that is not true in the \mathcal{T}_σ model) the amount of mixing it predicts is difficult to justify, particularly when one considers the source of energy for this mixing and the Richardson numbers at which it can occur; moreover large negative SGS heat fluxes are difficult to reconcile with the sense of the resolved flow, in that the co-spectrum of \overline{w} and $\overline{\theta}$ indicates that the small scale flux at the inversion becomes positive at small scales, e.g., Schumann (1991) and Stevens et al., (1999). The \mathcal{T}_σ model is also problematic, in that it makes the paradoxical statement that most of the flux is resolved, yet the SGS lengthscale is smaller than the grid-scale. Ultimately, however, it may have a useful artifact in that the ratio of the diagnostic, stability modified, lengthscale to the gridscale l_s/Δ might be a useful measure of our degree of confidence in the SGS model.

The \mathcal{S} models avoid the issue of fossil TKE inducing mixing. However, they do so at the expense of energy conservation. This is particularly true of the \mathcal{S}_δ model. This model is derived from a budget equation in which most of the adjustment of e to large-scale changes in the flow is accommodated by the mixing terms, but in being a diagnostic model it is implicitly assumed that this adjustment happens instantaneously through dissipation (i.e., the value of the SGS energy at two timesteps can change from a positive value to a zero value without any mixing having taken place.) The \mathcal{S}_σ model, on the other hand, is unsatisfactory in that it implicitly predicts long timescales for e but then proceeds to neglect the time-rate of change term.

In conclusion we wish to emphasize that in certain situations LES is sensitive to the SGS lengthscale formulation, and that at present we lack a good theory of how small scale turbulence forced by PBL-scale turbulent structures should behave at a strong capping inversion. This lack of understanding limits our ability to improve the SGS models.

References

- Deardorff, J. W.: 1973a, 'The use of subgrid transport equations in a three-dimensional model of atmospheric turbulence'. *J. Fluids Eng.* **95**, 429–438.
- Deardorff, J. W.: 1973b, 'Workshop on Micrometeorology'. In: D. A. Haugen (ed.): *Workshop on Micrometeorology*. Amer. Meteor. Soc., Chapt. Three-dimensional numerical modelling of the planetary boundary layer, pp. 271–311.
- Deardorff, J. W.: 1980, 'Stratocumulus-Capped Mixed Layers Derived from a Three-Dimensional Model'. *Bound.-Layer Meteor.* **18**, 495–527.
- Lilly, D. K.: 1967, 'The Representation of Small-Scale Turbulence in Numerical Simulation Experiments'. In: H. H. Goldstine (ed.): *IBM Scientific Computing Symposium on Environmental Sciences*. Yorktown Heights, N. Y., pp. 195–210. Order No. 320-1951.
- Moeng, C.-H. and J. C. Wyngaard: 1989, 'Spectral analysis of large-eddy simulations of the convective boundary layer'. *J. Atmos. Sci.* **45**, 3573–3587.
- Schemm, C. E. and F. B. Lipps: 1973, 'Some results from a simplified three-dimensional numerical model of atmospheric turbulence'. *J. Atmos. Sci.* **33**, 1021–1041.
- Schmidt, H. and U. Schumann: 1989, 'Coherent structure of the convective boundary layer derived from large-eddy simulations'. *J. Fluid Mech.* **200**, 511–562.
- Schumann, U.: 1991, 'Subgrid Length-Scales for Large-Eddy Simulation of Stratified Turbulence'. *Theoret. Comput. Fluid Dynamics* **2**, 279–290.
- Sommeria, G.: 1976, 'Three-Dimensional simulation of turbulent processes in an undisturbed trade wind boundary layer'. *J. Atmos. Sci.* **33**, 216–241.
- Stevens, B., C.-H. Moeng, and P. P. Sullivan: 1999, 'Large-eddy simulations of radiatively driven convection: sensitivities to the representation of small scales'. *J. Atmos. Sci.* **56**, in press.
- Sullivan, P., C.-H. Moeng, B. Stevens, D. H. Lenschow, and S. D. Mayor: 1998, 'Entrainment and structure of the inversion layer in the convective planetary boundary layer'. *J. Atmos. Sci.* **55**, 3042–3064.
- Sullivan, P. P., J. C. McWilliams, and C.-H. Moeng: 1994, 'A subgrid-scale model for large-eddy simulation of planetary boundary -layer flows'. *Bound.-Layer Meteor.* **71**, 247–276.